DIGITAL IMAGING FOR ROCK MASS CHARACTERIZATION

John Kemeny*+, Enock Mofya*+, Jim Holmlund^, and Steve Ahlgren^

*Dept. Mining and Geological Engineering, University of Arizona, Tucson, AZ 85721, kemeny@u.arizona.edu
+Split Engineering, 110 S. Church Suite 8312, Tucson, AZ 85701
^Geo-Map, Inc., 3323 N. Campbell, Tucson, AZ 85719

Abstract

Traditional methods for rock mass characterization in civil engineering applications include scanline surveying, cell mapping and geologic structure mapping. In spite of their importance, characterizing rock masses using these field methods is time-consuming, hazardous and prone to errors. This paper describes two new technologies for field fracture characterization: digital image processing of fracture traces, and laser-based imaging. These technologies offer the potential for gathering fracture and associated information in a semi-automatic or automatic fashion at a distance from the face. The automated procedures can reduce the errors associated with gathering field fracture data by eliminating human bias and by standardizing the sampling procedure. These automated procedures can also be used to increase the amount of fracture information that is routinely collected in a field survey. Also, by imaging rock faces from a distance, both safety and access problems are reduced or eliminated. Details of the two technologies are described in the paper. The two technologies offer synergies that may allow accurate fracture characterization to be carried out in a wide variety of field conditions. To investigate these two technologies, case studies have been carried out in Arizona and Colorado. The results of these studies indicate that both the image processing and laser-scanning methods are able to determine the 3D fracture orientations with a reasonable degree of accuracy. The laser-scanning technique is more accurate when imaging single faces but at the expense of more time in the field and additional hours to process the results. The digital imaging technique has the potential for being used in real time applications.

Introduction

Engineering in rock masses requires a detailed knowledge of site geology, structure, rock properties, hydrology, and other issues. Engineering disciplines that require an understanding of rock masses include the mining, civil, petroleum and environmental industries. A rock mass consists of intact rock separated by discontinuities. The discontinuities in the rock mass include faults, joints, bedding planes, and other types of fractures. With the exception of the small-scale frictional properties, the properties of the discontinuities must be determined in the field, from boreholes, excavations, and natural outcrops. Discontinuity properties to be determined in the field include orientation, length, spacing, roughness, persistence, aperture, filling, termination, and other properties (Priest, 1993).

Traditional methods for obtaining discontinuity data in the field include the scanline survey and cell mapping (Priest and Hudson, 1981; Priest, 1993). In the scanline survey, fracture information is collected along a line at a rock face. In cell mapping, the dominant structures (joint sets, faults, etc.) at the rock face are first identified and the average information (orientation, spacing, length, etc.) is then measured for each structure. Scanline surveys provide detailed information on the individual fractures in each set that can be used in probabilistic design, whereas cell mapping only provides average information about each joint set. On the other hand, cell mapping is far easier and less time consuming, and cell mapping can be conducted in situations where direct access to the face is not possible. In spite of their importance, characterizing rock masses in the field using either scanline surveys or cell mapping is difficult and prone to errors. First of all, there are large sources of error in gathering field discontinuity data with these methods, including sampling difficulties, choice of sampling method, human bias, instrument error, and many other problems. Secondly, there are the safety risks associated with conducting scanline or cell mapping surveys in the field. Rock faces are often unsafe due to loose rock at the base of the slopes and because of the potential for rockfall of blocks on the slopes. Finally, getting access to rock faces is often difficult or impossible.

Several new technologies offer the possibility of eliminating many of the problems with rock mass characterization described above. These include the technologies of digital imaging / digital image processing (Haralick and Shapiro, 1992; Russ, 1995) and laser-based imaging (Cyra Technologies, 2001). These technologies offer the potential for gathering fracture and associated information in a semi-automatic or automatic fashion at a distance from the face. In the first technology, digital images are taken of rock faces containing fractures. Image processing software is then used to delineate fracture traces in the images, and fracture properties (3D orientation, length, spacing, etc.) are extracted from the trace information using mathematical algorithms (Post et al., 2001). Several case studies utilizing the digital imaging approach have been conducted in Arizona and Colorado in the past year, and results from these case studies are described later in this paper. In the second technology, high-resolution laser-scanning devices are used to image rock faces containing fractures. The most useful for this purpose are the time-of-flight type of laser-scanners, which measure the time required for the laser beam to travel the distance to the rock face and back. These scanners produce a "point cloud" consisting of hundreds of thousands of individual distance measurements, the sum of which is a 3D rendering of the surface being scanned (Feng, 2001). Software is then used to extract 3D fracture properties. Each of these two technologies has advantages and disadvantages in different circumstances. Acquiring and processing still digital images is simple and straightforward when the surface being imaged is relatively flat (flat slope or wall of a pillar, for example). This technique is also amenable to automation, allowing a camera to be permanently installed on mine equipment for capturing rock face images continually. Laser-scanners, on the other hand, provide a very high-resolution 3D rendering of rock faces. These data can be used to extract accurate information on discontinuity orientation, spacing, size and shape. Laser-scanners are ideal for analyzing rough, complex, and messy rock faces. They are less ideal for relatively flat surfaces, since they rely on imaging actual fracture surfaces. At this time, laser-scanning is also not well suited for real-time applications since the scanning process takes several minutes (where the scanner must remain still) and at the present time processing the data can take several days. However, it is expected that laser-scanning equipment and associated software will become lighter, faster, and more user-friendly in the next several years.

The Digital Image Processing Approach for Rock Mass Characterization

This section describes image processing and mathematical algorithms that have been developed to extract three-dimensional fracture properties from digital images of fracture traces. Fracture traces are the resulting two-dimensional lineations on the digital image plane made by the imaging of three-dimensional discontinuities. An example of a digital image of a rock face and the resulting delineated fracture traces are shown in Figure 1a and 1b, respectively. Information about fracture traces that can be extracted with image processing software include trace orientation, length, spacing and large-scale roughness. Three-dimensional fracture properties that could be potentially extracted from the 2D trace information include orientation (strike and dip), true fracture spacing, and fracture size and shape. The most important three dimensional fracture properties are associated with fracture orientation. This includes the mean orientation of each joint set and some measure of the scatter about the mean orientation. A commonly used probability density function for joint orientation data that is adapted in this paper is the Fisher distribution (Fisher, 1953). This is a symmetric distribution about the mean orientation and uses a single parameter, the Fisher constant K.

The processing of a digital image of a rock face consists of the following steps:

1) Delineation of fracture traces in the digital images
2) Identifying joint sets by identifying clusters of trace angles
3) Determining the average orientation and a measure of the scatter for each joint set
4) Determining distributions for spacing, length and roughness for each joint set
5) Outputting the results

Details on each of these steps are described below.

The first step is to automatically delineate the fractures traces in the image, as shown in Figure 1b. At the University of Arizona and Split Engineering, algorithms for automatically delineating fracture traces have recently been developed, based on the Hough transform (Post et al., 2001; Post, 2001). The Hough

transform is a procedure that transforms a point in image space into a curve in parameter space using the relation:

$$\rho = x\cos\theta + y\sin\theta \qquad (1)$$

where ρ and θ represent the normal vector to the line passing through the image origin (Duda and Hart, 1972; Karnieli et al., 1996).

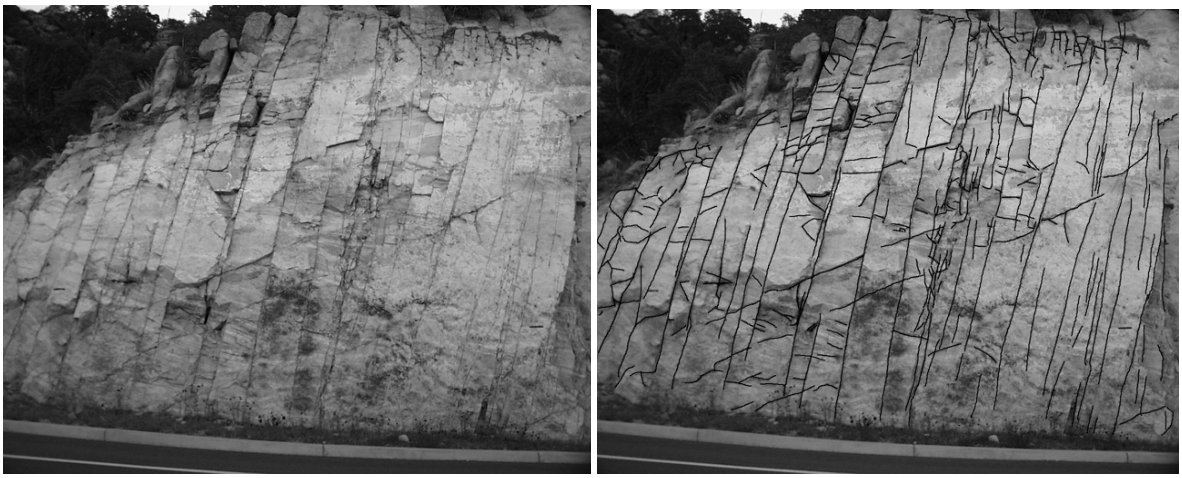

Figure 1. a) Image of a rock face showing fracture traces, b) delineation of the fracture trace.

This particular parameterization of the Hough Transform (HT) is often referred to as the RTHT where the R and T refer to ρ and θ. When the HT is performed on a binary image, each of the pixels other than the background is transformed to the parameter space. Each time a curve in parameter space passes through the same pixel, that pixel's value is incremented by 1 in the image (referred to as the accumulator image). Thus, bright points appear in the accumulator image at places where many curves intersect. That intersection corresponds to a strong linear feature in image space. In order to pick more than one line in an image, the curves corresponding to the strongest line must then be subtracted from the accumulator image, by subtracting from the accumulator the HT image of the line that was previously located. This procedure can be repeated to generate as many lines as desired. However, a simple method of automatically determining when to stop finding lines is to use a parameter called "cutoff". An example of the performance of the Hough Transform for different cutoff parameters is shown in Figure 2. Figure 2 demonstrates the success of the Hough transform in finding linear features. The Hough transform by itself does not preserve information on fracture length, but variations that perform the RTHT on subsets of the entire image have been developed by Mirmehdi and West (1991), Fitton and Cox (1998), Yacoub and Jolion, (1995) and Post et al. (2001). Once the fracture traces have been delineated, information about each trace can be determined, including trace angle, length, spatial location, and roughness. The trace angle information is then used to cluster the traces into a number of different sets. Further analysis of the trace information is thereafter conducted separately for each joint set.

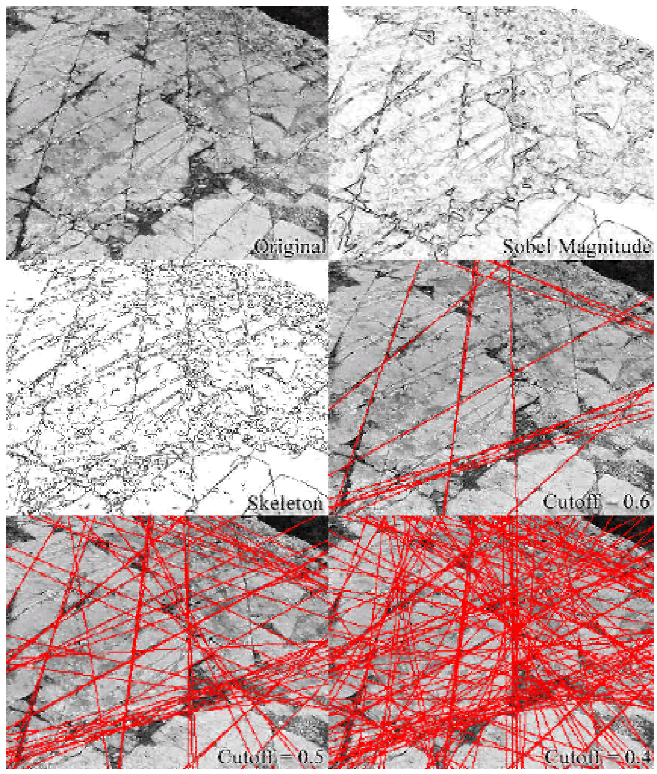

Figure 2. Example of the Hough Transform and the effect of the cutoff parameter. Some standard filtering of the image is conducted before the Hough transform is performed.

The second step is to extract three dimensional fracture properties from the fracture trace information. First of all, mathematical relationships have been developed between the normal to a joint plane, the orientation of a rock face that the joint intersects, and the resulting trace angle made by the joint on the rock face. These relationships also take into account the angle between the normal to the rock face and the axis of the camera. These are straightforward mathematical relationships based on vector calculus, and they are described in Post et al. (2001) and Post (2001). Secondly, an assumption is made about the distribution of joint orientations within a set, namely that they resemble a Fisher distribution (Fisher, 1953). The Fisher distribution function gives the probability per unit angular area of finding a direction within an angular area dA centered at an angle θ from the true mean:

$$f(\theta) = \frac{Ke^{K\cos(\theta)}}{2\pi(e^{K} - e^{-K})} \tag{2}$$

where K is the Fisher constant. This is a symmetric distribution about the mean orientation, and as expected, the distribution has a maximum at the true mean ($\theta = 0$). A large K predicts a distribution more strongly concentrated about the true mean. Typical K values for rock joints within a set range from 20 to 300. As an example, Figure 3 presents data on a joint set with a mean dip direction of 125 and a mean dip of 60. Figures 3a and 3b are lower hemisphere, equal angle plots of normal vectors for K = 20 and K = 100, respectively. The squares in the figures are the computer generated picks from the Fisher distribution and the triangle in each figure is the mean orientation. The computer-generated picks from the Fisher distributions were calculated using relationships given in Priest (1993).

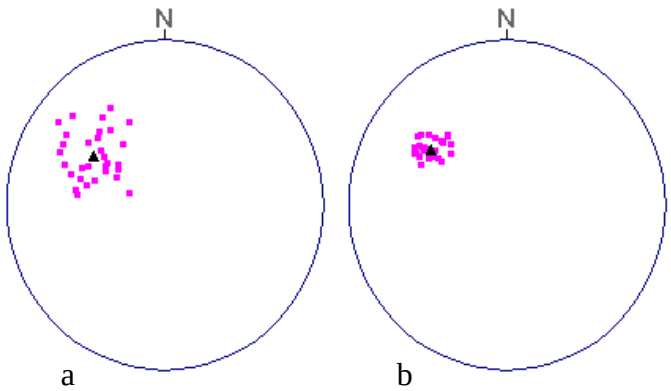

Figure 3. Lower hemisphere, equal angle plots for a joint set with a mean dip of 60 and a mean dip direction of 125 degrees. a) K = 20, b) K = 100.

A forward problem can now be defined where a distribution of joint orientations is given (mean dip, mean dip direction and Fisher constant K) and the resulting trace angles on a rock face of a given orientation (dip and dip direction) can be calculated. As an example, consider the joint orientation distributions shown in Figure 3b. Using the mathematical relationships described above, the resulting trace angle distributions for two rock faces are shown in Figure 4, the first one for an E-W face dipping 85 degrees to the South, and the second one a N-S face dipping 80 degrees to the East (in both cases the axis of the camera rises 10 degrees from horizontal). The results show that on the N-S face, the traces have a mean rake of 55.05 degrees with a standard deviation of 7.05, while on the E-W face, the traces have a mean rake of 129.9 with a standard deviation of 9.56 (rake is the clockwise angle made by the trace in the plane of the face measured from horizontal).

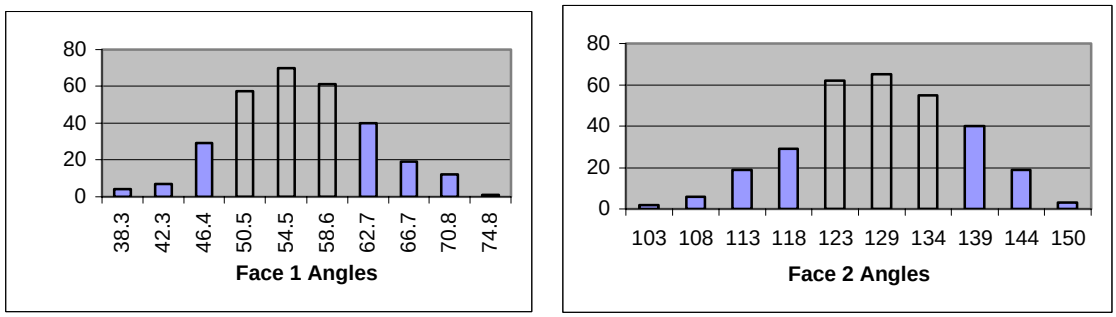

Figure 4. Distribution of trace angles on an E-W face (a) and a N-S face (b) for a joint set with a mean dip of 60, mean dip direction of 125, and a Fisher constant of 100.

The example given above is a forward problem where the actual joint set orientation is known and the trace angles are predicted. The actual problem we want to solve is the inverse of this problem, where the distribution of trace angles for a joint set on one or more faces is known (mean, standard deviation, skewness, etc.), and the parameters for the joint set that gave those results (mean dip, mean dip direction, and the Fisher K constant) must be estimated. A type of genetic algorithm called Differential Evolution forms the basis for the inverse routine for the proposed work (Price and Storn, 1997). The goal of the Differential Evolution (DE) is to find the optimum mean dip, mean dip direction, and Fisher K constant that match an observed distribution of fracture trace angles. Each input “chromosome” will have three “genes”, the previously mentioned joint parameters. After each iteration, the error for each chromosome is computed, with the chromosome with the lowest error surviving to the next iteration. Also, the chromosomes undergo mutation and recombination to produce a secondary vector, as described in Post (2001) and also illustrated in Figure 5. After each iteration, an average error for the entire population of the new primary vector is computed. If that population error is less than the user-defined threshold, or if the number of generations reaches some maximum, then the DE algorithm is stopped. The

chromosome with the lowest error is selected from the primary vector and the three dimensional joint parameters for the image traces have been found.

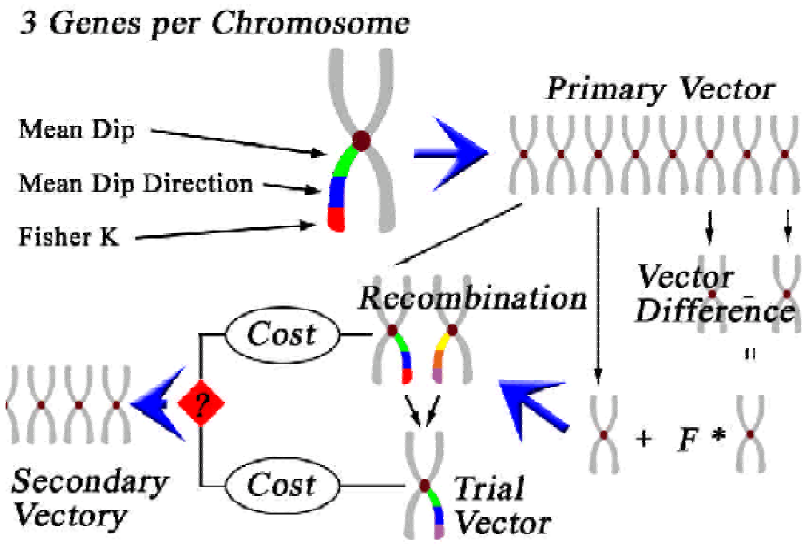

Figure 5. Overview of the differential evolution algorithm.

As an example, consider the same joint set and rock face parameters as shown in Figures 3b and 4, however in this case we start with the trace information on the rock faces (mean trace angle, standard deviation of the trace angles) and make predictions about the actual orientation of the joint set (mean dip, mean dip direction, and Fisher constant K). In this case information from both the EW and NS rock faces are used, and no a-priori information is assumed about the range of dip or dip direction. Thus the search range for dip is 0-90, for dip direction is 0-359, and for K is 10-300. After 52 iterations of the DE algorithm the error function converges to a low value, and the chromosome with the lowest error has a mean dip of 60.3, mean dip direction of 125.76, and a mean K of 102.42. These results are very close to the actual values of 60, 125 and 100. The “error surface” for this case is shown in Figure 6a (for a fixed K = 100). For a given set of trace angle data, the value of a point on the error surface represents the error between trace angles measured and those predicted for that dip and dip direction. A point with low error indicates a good match between calculated and measured trace angles and therefore a likely candidate for the correct 3D joint set orientation. The error surface shown in Figure 6a shows a kind of “bull’s eye” shape to the error surface, and as expected, the DE algorithm can quickly converge to the red point at the center of the bulls eye, which has dip=60 and dip direction = 125. Additional case studies have shown that the DE algorithm can predict joint orientations within one degree of the actual even if the two rock faces differ in strike by as little as 15 degrees.

If the DE algorithm is used with trace information from only one of the two faces, the DE algorithm does not consistently converge to the same dip, dip direction and K. The error surface for this case is shown in Figure 6b. In this case, the colored pixels (the pixels representing the 5 lowest levels of error) form a wide band representing dip directions from 40 to 140. However, looking closely at the pixels in this zone, red pixels representing the lowest error occur in two neighborhoods, one around a dip direction of 120 and the other around a dip direction of 55. This agrees with the DE evolution results, where the algorithm converged in these same two neighborhoods. Within each neighborhood, the dip is constrained within one or two degrees but the dip direction varies by 5-10 degrees in either direction. If a rough estimate of the average orientation of the joint set is known a priori (say, from a geologic model), then one of these neighborhoods could possibly be eliminated, and the orientation could be predicted within 10 degrees. This could be satisfactory for some purposes, say in the estimation of rock blastability for a road cut. However, it might not be satisfactory for slope stability applications. The shape of the error surface for the case of a single rock face can take many forms, including some that have multiple “bull’s eyes”

rather than a single broad surface as shown in Figure 6b. Additional simulations with single rock face imaging will be the topic for future studies.

The technique described above has obvious applications for rock mass characterization for a number of civil applications, including roadways, bridge foundations and dam foundations.

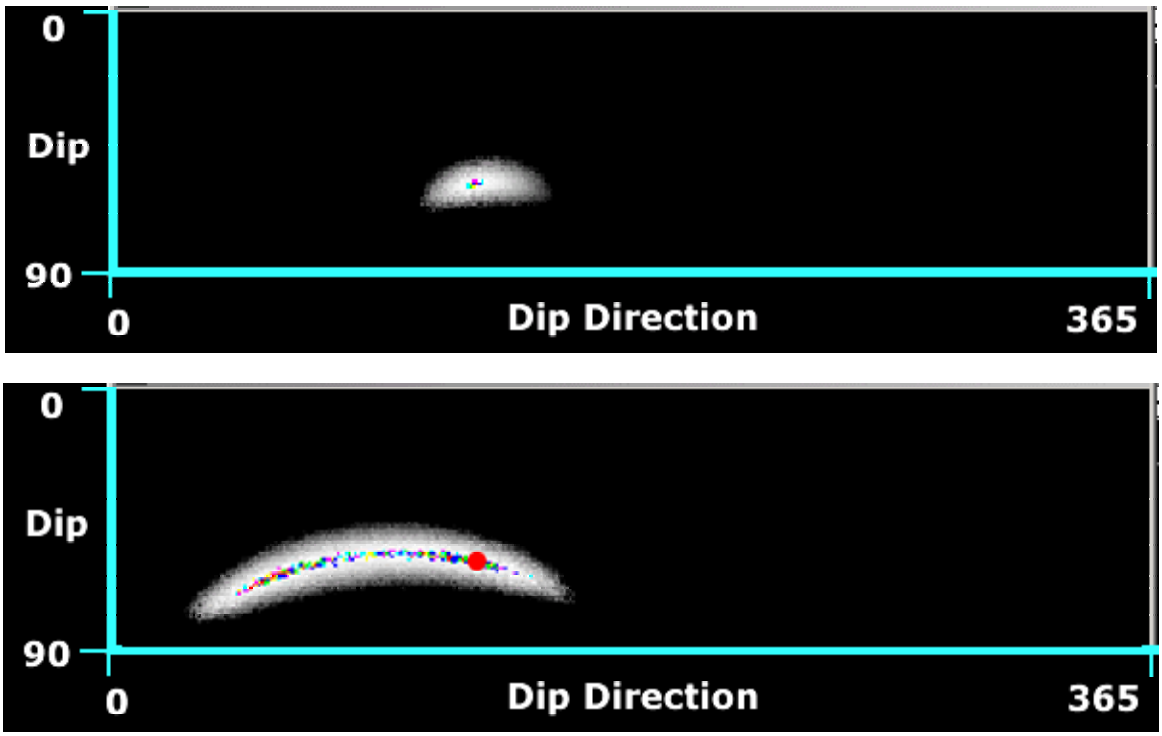

Figure 6. Error surface plot at a constant K of 100. Errors range from low (white) to high (black). The lowest 5 levels of error are colored, with red being the very lowest level of error. a) error surface using trace information from two non-parallel faces, b) error surface using trace information from only a single face. The correct solution in b) is marked by the large red dot.

Case Studies with the Digital Imaging Approach

A number of field case studies have been conducted to assess the accuracy of the digital image processing technology method on actual field situations. Field case studies have been conducted on natural rock outcrops, blasted road cuts and blasted mine benches. Field case studies have been conducted in sandstone, basalt, slate, granite and gneiss. The results from two of the case studies near Crested Butte, Colorado are described below.

The first case study is located near Daisy Pass, which is about 10 miles north of Crested Butte. The rock type here is a heavily jointed slate. The second case study is located near the town of Almont, which is about 15 miles south of Crested Butte. The rock type here is sandstone. Some rock outcrop images from the Daisy Pass and Almont case studies are presented in Figure 8a and 8b, respectively. Images for both case studies were taken with a Sony DSC-S75 digital camera set at a resolution of 1280 by 960 pixels. All images were taken with the camera aimed perpendicular to the strike of the rock outcrops but not the dip. The fracture traces in the images were delineated using hand-editing tools in the NIH Image public-domain program (Rasband, 1998), and the trace angles were measured using built in functions in this program. The traces were separated into the different sets, one for each joint set. At the Daisy Pass site only one joint set was analyzed, and at the Almont site 2 joint sets were analyzed. These trace angles were then directly input into the Differential Evolution algorithm to estimate the mean dip, mean dip direction and Fisher K for each of the joint sets. The results are presented in Table 1. The check against

the actual results was made using two methods. For the Daisy Pass study, scanline surveys were conducted, which were used to calculate the actual mean dip, dip direction, and K. For the Almont study, cell mapping was utilized to estimate the average dip and dip direction for each of the joint sets. In this case the actual value for the Fisher constant K could not be determined. The scanline and cell mapping results are also shown in Table 1.

Figure 7. Images from two case studies carried out near Crested Butte, Colorado. a) Daisy Pass case study in slate, b) Almont case study in sandstone.

Table 1 shows that for the Daisy Creek study, the analysis of fracture traces was able to predict the dip within one degree and the dip direction within 4 degrees. The K factor, however, differed by a larger amount (K=89 from scanline data, K=230 from trace analysis). For the Almont study, the predicted dip and dip directions for the two joint sets were close except in one case (dip direction for joint set 1). K values were predicted but not measured since only cell mapping was conducted at this site.

	Daisy Pass	Almont	
	Set 1	Set 1	Set 2
Actual Dip	64	53	7
Predicted Dip	63	58	12
Actual Dip Direction	338	270	215
Predicted Dip Direction	342	252	216
Actual K	89	N/A	N/A
Predicted K	230	144	150

Table 1. Results from two case studies conducted near Crested Butte, Colorado.

The results of these two field case studies indicate higher errors than those from the synthetic case studies described previously. This is to be expected, since errors can occur in a number of measured quantities, and deviations from the assumptions made in the analysis occur (the assumption that the rock faces are flat, for instance). First are possible errors in the measured quantities, including the orientations of the rock face and the camera. Secondly, the computer algorithms assume that the rock face is flat, which is a good assumption for the Daisy Pass study but not the Almont study. A third problem is the difference in the surface area taken from photos versus that from the scanline surveys. In general digital images were taken of an entire face while only the bottom part of the face was accessible for scanline data. This also affected the number of fractures measured in the scanline surveys as opposed to the face imaging. Fourth, a major assumption is that the joint orientations can be described by a Fisher distribution. Steeply dipping joint sets often show very little variation in dip compared to the variation in dip direction, thus not adhering to one of the basic assumptions of a symmetric distribution. In the future, non-symmetric distributions could be considered, though these will have at least one additional unknown parameter to be determined. Finally, orientation bias was not considered in the analysis of the data

(Priest, 1993). No correction for bias is needed in the computer-generated case studies, since all picks from the Fisher distribution appear on the "virtual rock face". There is expected to be bias, however, in the scanline results and the rock face imaging results. The effect of orientation bias will be considered in the future. The case studies conducted thus far cannot be used to pinpoint the source of error from those discussed above. Additional case studies will be conducted for the purpose of providing insight into the specific sources of error.

Emerging Technology: Laser Scanning for Rock Mass Characterization

Even though laser scanners have been around for a number of years, it is only recently that their accuracy and ease of use have reached the point where they can provide accurate information on 3D fracture properties. The most useful for this purpose are the time-of-flight type of laser-scanners, which measure the time required for the laser beam to travel the distance to the rock face and back. These scanners produce a "point cloud" consisting of hundreds of thousands of individual distance measurements, the sum of which is a 3D rendering of the surface being scanned. For example, the Cyrax 2400 laser scanner (CYRA technologies, 2001) can capture up to 800 measurement points per second over a 40º x 40º field-of-view, with 6mm positional accuracy at a range of over 50 meters. In a typical 5-10 minute scan the scanner captures and stores as many as 480,000 points. The point cloud data can then be processed in a relatively straightforward manner to determine the orientation of individual discontinuity surfaces, using either software provided by the manufacturer or specialized software developed by the user. A picture of the Cyrax laserscanner being used for rock mass characterization at an open-pit mine in Arizona is shown in Figure 8.

Figure 8. Cyrax laser scanner being used for rock mass characterization at a mine in Arizona.

The procedure for characterizing fracturing in a rock mass using 3D laser-scanners consists of the following five steps:

1) Surveying in a number of control points
2) Scanning the rock face using the 3D laser-scanner
3) Transforming the laser scanning point cloud to the surveyed coordinate system
4) Determining fracture orientation and other fracture properties from the transformed point cloud data
5) Outputting the results into a suitable database

Details on these steps can be found in Feng (2001) and Gordon et al. (2001).

A number of groups are presently utilizing laser scanners for rock fracture characterization (Ahlgren et al., 2001). They, as well as others, have concluded that 3D laser-scanners have a large potential in this regard. For instance, a recent doctoral dissertation investigated three novel methods for extracting 3D fracture information from exposed rock faces: geodetic total station, close-range photogrammetry, and 3D laser-scanners (Feng, 2001). Of the three methods, they concluded that 3D laser-scanners had the highest potential for characterizing fractures in a semi-automatic fashion. The primary drawbacks with laser-scanners included their cost, weight, time-to-scan, and the fact that some surveyed points are needed as a base for the results. There are synergies between the laser scanning technology and the digital imaging technology described previously. For example, very complex rough rock faces may present challenges to the camera-based imaging technology while being optimal conditions for the laser scanning technology. In such a situation, the trace delineation algorithms can still provide valuable information on the location and outline of fracture surfaces, which can then be used to optimize the processing of the point cloud data to characterize the fractures. On the other hand, a smooth face is ideal for the image processing technology while not providing any useful information from the laser scanning technology (since individual fracture surfaces cannot be seen). The laser scanning technology is also not appropriate for situations where real-time continuous measurements are desired.

Conclusions

This paper described two new technologies for rock fracture characterization. In the first technology, an image processing approach has been developed for estimating three-dimensional fracture orientations from two-dimensional fracture trace information gathered from exposed rock faces. In this approach digital images are taken of rock faces, and these images are processed using digital image processing routines to delineate the fracture traces. The trace angle distribution for each joint set is then determined. The approach assumes that the fractures occur in sets, and that each set can be described by a mean orientation and a measure of the scatter about the mean. In this paper we assume a Fisher distribution of joint orientations and utilize the Fisher constant K as a measure of scatter. Mathematical relationships are developed that relate the 3D fracture properties with the trace angles that would be measured on one or more rock faces. These algorithms are used in conjunction with a genetic algorithm to invert the trace angles to estimate 3D joint orientation. A number of case studies have been conducted to assess the accuracy of the method. Synthetic case studies involving only computer-generated data indicate that if trace angles from two non-parallel faces are used, the prediction of 3D fracture orientation is very accurate (less than one degree error), even if the faces differ by as little as 15 degrees. The synthetic case studies also indicate that fairly accurate predictions can be made (less than 5 degrees error) in certain circumstances even if the trace angles from only a single face are used. Overall, the techniques developed in this paper show a great potential for determining 3D fracture properties from 2D digital images.

In the second technology, high-resolution laser-scanning devices are used to image rock faces containing fractures. The most useful for this purpose are the time-of-flight type of laser-scanners, which measure the time required for the laser beam to travel the distance to the rock face and back. These scanners produce a “point cloud” consisting of hundreds of thousands of individual distance measurements, the sum of which is a 3D rendering of the surface being scanned (Feng, 2001). Software is then used to extract 3D fracture properties.

Overall, the two techniques described in this paper show a great potential for determining 3D rock fracture properties for a number of civil applications, including roadways, bridge foundations, dam foundations and tunneling.

Acknowledgements

This work is supported under Split Engineering NSF SBIR Phase I contract DMI-0128392. Special thanks are given to Jason Elliason for participating in the Crested Butte field studies described in the paper.

References

Ahlgren, S., Holmlund, J., Nicoli, J. and P. Griffiths. 2001. Integrating laser scanning and 3D visualization for semi-automated fracture detection and analysis (abstract), GSA Annual Meeting, Boston, MA.

Cyra Technologies. (2001). http://www.cyra.com

Duda, R.O. and Hart, P.E. (1972). Use of the Hough transform to detect lines and curves in pictures, Commun. ACM, 15:11-15.

Feng, Q. (2001). Novel Methods for 3D semi-automatic mapping of fracture geometry at exposed rock faces, Doctoral Thesis, Royal Institute of Technology, Stockholm, Sweden.

Fisher, R. 1953. Dispersion on a sphere. *Proc. Royal Soc. Londo*n, A217, 295-305.

Fitton, N.C. and Cox, S.J.D. 1998. Optimising the application of the Hough transform for automatic feature extraction from geoscientific images. *Computers and Geosciences* 24(10): 933-951.

Gordon, S., Lichti, D. and M. Stewart. 2001. Application of a high-resolution ground-based laser scanner for deformation measurements, Proc. FIG10 Symp., Orange, CA.

Haralick, R.M. and Shapiro, L.G. (1992). Computer and Robot Vision, Addison-Wesley Publishing, Reading, Mass.

Karnieli, A., Meisels, A., Fisher, L. and Arkin, Y. 1996. Automatic extraction and evaluation of geological linear features from digital remote sensing using a Hough transform. *Photogrammetric Engineering and Remote Sensing* 62(5): 525-531.

Kemeny, J., Murphy, R. and Post, R. 2000. Use of fracture traces on digital images of rock faces for 3D rock characterization and probabilistic slope design (abstract), GSA Annual Meeting, Reno, NV.

Mirmehdi, M., West, G. and Dowling, G. 1991. Label inspection using the Hough transform on transputer networks. *Microprocessors and Microsystems* 15(3): 167-173.

Post, R. (2001). Characterization of joints and fractures in a rock mass using digital image processing, M.S. Thesis, University of Arizona, Tucson.

Post, R., Kemeny, J., and Murphy, R. (2001). Image processing for automatic extraction of rock joint orientation data from digital images, Proceedings 38th US Rock Mech. Symp., Washington, D.C., A.A. Balkema, Rotterdam.

Price, K. and Storn, R. 1997. Differential Evolution. *Dr. Dobb's Journal* 22(4): 18-24,78.

Priest, S. D. (1993) Discontinuity Analysis for Rock Engineering, London, Chapman & Hall.

Priest, S.D. and Hudson, J.A., Estimation of discontinuity spacing and trace length using scanline surveys, International Journal of Rock Mechanics, Mining Science & Geomechanics Abstracts, 1981, 18, 183-197.

Rasband, W. (1998). NIH Image, an image processing program, http://rsb.info.nih.gov/nih-image/.

Russ, J.C. (1995). The Image Processing Handbook, CRC Press.

Yacoub, S.B., and Jolion, J.M. (1995). Hierarchical line extraction, Poce. Image Sig. Proc, 142:7-14.